



QSAR development and profiling of 72,524 REACH substances for PXR activation and CYP3A4 induction

Abildgaard Rosenberg, Sine; Xia, M.; Huang, R.; Nikolov, Nikolai Georgiev; Wedebye, Eva Bay; Dybdahl, Marianne

Published in:
Computational Toxicology

Link to article, DOI:
[10.1016/j.comtox.2017.01.001](https://doi.org/10.1016/j.comtox.2017.01.001)

Publication date:
2017

Document Version
Publisher's PDF, also known as Version of record

[Link back to DTU Orbit](#)

Citation (APA):
Abildgaard Rosenberg, S., Xia, M., Huang, R., Nikolov, N. G., Wedebye, E. B., & Dybdahl, M. (2017). QSAR development and profiling of 72,524 REACH substances for PXR activation and CYP3A4 induction. *Computational Toxicology*, 1, 39-48. <https://doi.org/10.1016/j.comtox.2017.01.001>

General rights

Copyright and moral rights for the publications made accessible in the public portal are retained by the authors and/or other copyright owners and it is a condition of accessing publications that users recognise and abide by the legal requirements associated with these rights.

- Users may download and print one copy of any publication from the public portal for the purpose of private study or research.
- You may not further distribute the material or use it for any profit-making activity or commercial gain
- You may freely distribute the URL identifying the publication in the public portal

If you believe that this document breaches copyright please contact us providing details, and we will remove access to the work immediately and investigate your claim.



QSAR development and profiling of 72,524 REACH substances for PXR activation and CYP3A4 induction



S.A. Rosenberg^a, M. Xia^b, R. Huang^b, N.G. Nikolov^{a,1}, E.B. Wedebye^{a,1}, M. Dybdahl^{a,*,1}

^a Division of Diet, Disease Prevention and Toxicology, National Food Institute, Technical University of Denmark, Mørkhøj Bygade 19, 2860 Søborg, Denmark

^b National Center for Advancing Translational Sciences, National Institutes of Health, 9800 Medical Center Drive, Rockville, MD 20850, USA

ARTICLE INFO

Article history:

Received 21 November 2016

Received in revised form 16 January 2017

Accepted 19 January 2017

Available online 24 January 2017

Keywords:

PXR

CYP3A4

QSAR

REACH

Screening

ABSTRACT

The Pregnane X Receptor (PXR) is a key regulator of enzymes, for example the cytochrome P450 isoform 3A4 (CYP3A4), and transporters involved in the metabolism and excretion of xenobiotics and endogenous compounds. Activation of PXR by xenobiotics causes altered protein expression leading to enhanced or decreased turnover of both xenobiotics and endogenous compounds. This can potentially result in perturbations of normal physiology and adverse effects. Identification of PXR activating and CYP3A4 inducing compounds is included in drug-discovery programs but we still need similar information for the remaining tens-of-thousands of man-made compounds to which humans are potentially exposed. In the present study, we used high-throughput *in vitro* assay results for 2816 drugs to develop four quantitative structure-activity relationship (QSAR) models with binary outputs for binding to the human PXR ligand binding domain, full-length human and rat PXR activation and human CYP3A4 induction, respectively. Rigorous cross- and blinded external validations demonstrated four robust and highly predictive models with balanced accuracies ranging from 75.4% to 92.7%. The models were applied to screen 72,524 substances pre-registered under the EU chemicals regulation, REACH, and the models could predict 52.5% to 71.9% of the substances within their respective applicability domains. These predictions can, for example, be used for priority setting and in weight-of-evidence assessments of chemicals. Statistical analyses of the experimental drug dataset and the QSAR-predicted set of REACH substances were performed to identify similarities and differences in frequencies of overlapping positive results for PXR binding, PXR activation and CYP3A4 induction between the two datasets.

© 2017 The Authors. Published by Elsevier B.V. This is an open access article under the CC BY-NC-ND license (<http://creativecommons.org/licenses/by-nc-nd/4.0/>).

1. Introduction

The nuclear receptor (NR) superfamily is a large group of transcription factors that control expression of multiple genes involved

in a broad range of biological processes, such as development, homeostasis and metabolism. The transcriptional activity of NRs is primarily regulated through ligand binding [1]. The Pregnane X Receptor (PXR), first described by Kliewer and colleagues in 1998, is a member of the NR superfamily [2,3]. PXR is mainly expressed in the liver, intestine and kidneys, and plays a key role in the regulation of genes involved in the metabolism and efflux of endogenous hormones and xenobiotic molecules [3–5]. The genes regulated by PXR include genes encoding enzymes, such as cytochrome P450s (CYPs), glucuronyltransferases and sulfotransferases, as well as transporters, such as P-glycoprotein and multidrug resistance proteins [2,3,6–8]. The ligand-binding domain (LBD) of PXR is large and flexible, and can change its shape to accommodate structurally diverse molecules including steroids, bile acids, antibiotics, statins, and pesticides [9,10]. A considerable amount of inter-species variation has been observed in the PXR LBD with human, rabbit and rat sharing roughly 75–80% amino acid identity [11,12]. There are numerous examples of differences in ligand binding to PXR and resulting downstream transcription

Abbreviations: AD, applicability domain; AOP, adverse outcome pathway; CYP, cytochrome P450; CYP3A4, human cytochrome P450 isoform 3A4; DTU, Technical University of Denmark; Food, National Food Institute; hPXR, full-length human Pregnane X Receptor; hPXR-LBD, human Pregnane X Receptor Ligand Binding Domain; IATA, Integrated Approaches to Testing and Assessment; LBD, Ligand Binding Domain; LPDM, Leadscape® Predictive Data Miner; NCATS, National Center for Advancing Translational Sciences; NIH, National Institute of Health; NR, nuclear receptor; PLR, partial logistic regression; PRS, Pre-Registered Substances; PXR, Pregnane X Receptor; QSAR, quantitative structure-activity relationship; qHTS, quantitative high-throughput screening; REACH, Registration, Evaluation, Authorisation & restriction of Chemicals; rPXR, full-length rat Pregnane X Receptor; RXR α , Retinoid X Receptor α ; SD, standard deviation; TR-FRET, time-resolved fluorescence resonance energy transfer; XRE, Xenobiotic Response Element.

* Corresponding author.

E-mail address: mdyb@food.dtu.dk (M. Dybdahl).

¹ Contributed equally.

<http://dx.doi.org/10.1016/j.comtox.2017.01.001>

2468-1113/© 2017 The Authors. Published by Elsevier B.V.

This is an open access article under the CC BY-NC-ND license (<http://creativecommons.org/licenses/by-nc-nd/4.0/>).

of enzymes and transporters between species, which complicates the extrapolation of results from *in vivo* animal studies to humans [11,13–15].

PXR is located in the cytoplasm and translocated to the nucleus upon ligand binding, and here the PXR-ligand complex heterodimerizes with the Retinoid X Receptor alpha (RXR α), another member of the NR superfamily. The PXR-RXR α heterodimer complexes with co-activators, and this multi-protein complex binds to the Xenobiotic Response Element (XRE) in the promoter region of target genes and induces their transcription leading to altered expression of their encoded proteins [2,3,16]. Because many of the proteins regulated by PXR are not only involved in the metabolism and transport of xenobiotics, but also of various endogenous compounds such as steroid and thyroid hormones, an altered protein expression upon xenobiotic exposure may interfere with the homeostatic balance of such endogenous compounds [17,18]. This interference can potentially affect normal physiological functions [2,19] and may result in adverse health effects. Findings from previous studies indicate that there is an association between PXR activation by environmental chemicals and adverse health effects [15,18,20,21]. The importance of PXR activation is also reflected in a number of suggested adverse outcome pathways (AOPs) available from the online AOP-Wiki [22], for example an AOP describing how activation of PXR and other related NRs upregulate thyroid hormone catabolism resulting in hypothyroidism and subsequent adverse neurodevelopmental outcomes [23]. The AOPs are envisioned to promote the industry's and regulators' use of results from alternative methods such as *in vitro* tests and computational models in chemical risk assessments to reduce, refine or replace traditional animal tests [24–26], for example by applying the AOP in an Integrated Approaches to Testing Assessment (IATA) context to support regulatory decisions [27].

PXR is also known to be involved in drug-drug interactions in which an administered drug affects the metabolism and excretion of a co-administered drug, leading to decreased efficacy or increased toxicity [2,28,29]. For this reason, attenuation of PXR activity has become an important focus area in early drug-discovery programs [30]. Similar to drug-drug interactions, an altered expression of enzymes and transporters through PXR activation upon xenobiotic exposure may cause changes in the response to other xenobiotic compounds.

Among the many PXR target genes is the gene encoding CYP3A4, an oxidizing enzyme involved in phase I metabolism of various compounds [4,31]. CYP3A4 is considered the main drug-metabolizing CYP isoform in the human liver and is involved in the metabolism of more than 50% of drugs on the market [2,5]. In most cases, CYP3A4 causes chemicals to become less biologically active and promotes their excretion; but in other cases it has the opposite effect causing bioactivation by converting them to metabolites that are more toxic than the parent molecule [32].

Because xenobiotic activation of PXR has the potential to alter normal physiology and lead to adverse effects, it is of great importance to identify chemicals that may act through this mechanism. In a study from 2011, Shukla and colleagues used four high-throughput *in vitro* assays to profile more than 2800 clinically-used and investigational drugs for their ability to bind to the human PXR-LBD, activate full-length human and rat PXR, and induce human CYP3A4 [14]. Chemicals in the ToxCast program [33], which include both drugs and environmental chemicals, have also been tested for these mechanisms in related assays [34]. However, we still need similar information for the remaining tens-of-thousands of xenobiotics to which humans are potentially exposed [35,36].

In the present study, we used the high-throughput *in vitro* data from Shukla et al. [14] to train and validate four Quantitative Structure-Activity Relationship (QSAR) models for human PXR-

LBD binding, human and rat PXR activation, and human CYP3A4 induction, respectively. QSAR models are computational models that relate chemical structures to, e.g., a biological activity, and they can be used to predict the activity of an untested chemical based on its chemical structure (an introduction to QSAR can e.g. be found in [37,38]). In general, QSARs are rapid and cost-effective tools for predicting biological activities of chemical structures and can be used for virtual screening of single substances as well as large chemical inventories. The four developed models were applied to screen a structurally diverse library of 72,524 chemicals from the EU chemicals regulation REACH (Registration, Evaluation, Authorisation and Restriction of Chemicals) list of Pre-Registered Substances (PRS) [39,40], containing substances potentially present in our food, the environment and consumer products. These QSAR predictions can, e.g., be used, possibly together with other relevant data, 1) to identify and prioritize chemical substances for further testing and 2) in an IATA context, together with relevant AOP(s), to guide further testing and regulatory decisions in chemical risk assessments [25,27,41]. Furthermore, statistical analyses of the experimental drug dataset and the QSAR-predicted REACH PRS set were performed in order to elucidate similarities and differences in co-occurrences of overlapping positive results for PXR binding, PXR activation and CYP3A4 induction between the two chemical universes.

2. Materials and methods

2.1. Experimental datasets

We used four datasets containing chemical structure information and *in vitro* experimental data for a collection of 2816 clinically-used and investigational drugs to train and validate the QSAR models. The experimental data of the 2816 compounds included results from quantitative high-throughput screening (qHTS) for binding to the LBD of human PXR at the protein level (hPXR-LBD); activation of full-length human PXR (hPXR) and full-length rat PXR (rPXR) at the cellular level; and induction of human CYP3A4 at the cellular level (CYP3A4). All experimental data were generated by the National Center for Advancing Translational Sciences (NCATS) at the National Institute of Health (NIH). The compound collection, qHTS assays, and the classification of the qHTS results into actives, inconclusives and inactives have been described previously [14,42,43]. Briefly, actives showed binding to the hPXR-LBD, activation of hPXR and/or rPXR and/or induced transcription of CYP3A4 according to the applied assays. Inactives did not show activity in the given assay, and inconclusives showed equivocal activity results in the assays. Only the substances in each dataset classified as either active or inactive were used, i.e. substances with inconclusive experimental results were excluded. The experimental results for about one third of the substances in each of the four main datasets were masked by NIH NCATS and these compounds were used as external test sets for blinded external validations after the model development was finished. The selection of the test sets was designed and made by NIH NCATS scientists, who clustered all compounds in the dataset on structural similarity using the Euclidian distance and then, within each structure cluster and for each of the four endpoints, approximately one-third actives and one-third inactives were selected randomly. Thus the training and test sets are structurally comparable and have similar distributions of actives and inactives. NIH NCATS sent the training sets containing structure information and experimental results and the test sets containing only structure information to the National Food Institute (Food) at the Technical University of Denmark (DTU), who performed the structure preparations, the

model development and validations as well as the virtual screenings.

Furthermore, a dataset containing ~4000 additional compounds with experimental data from the qHTS assay for hPXR-LBD was used for supplementary performance assessment of the developed hPXR-LBD QSAR model [20,43].

2.2. Structural preparation of the datasets

The commercial QSAR software applied in this study can handle organic chemical substances with a known and unambiguous 2D structure. We apply an overall definition of substances acceptable for QSAR processing in all our in-house QSAR software [44,45], as substances:

- containing at least two carbon atoms
- containing only H, Li, B, C, N, O, F, Na, Mg, Si, P, S, Cl, K, Ca, Br, and/or I
- that are not mixtures containing two or more organic components

Substances that did not fulfil these criteria were removed from the datasets. Further processing of the structural information included dissociation simulation and subsequent neutralization of the structures, i.e. all substances were used in their non-ionized form. An overview of the number of QSAR-ready substances in the final training and external test sets after structure preparation can be found in Table 1. These sets are available upon request.

2.3. QSAR modeling

We used the commercial software, Leadscope® Predictive Data Miner (LPDM), a component of Leadscope® Enterprise Server version 3.2.4 [46], to build the four QSAR models. Briefly, LPDM calculates nine molecular descriptors (AlogP, Hydrogen Bond Acceptors and Donors, Lipinski Score, Molecular Weight, Parent Atom Number, Parent Molecular Weight, Polar Surface Area, Rotatable Bonds) for each chemical structure in the training set and performs a systematic sub-structural analysis using a template library of more than 27,000 predefined structural features [47]. The molecular descriptors and structural features are included in a default initial descriptor set. In addition, the system can generate and add training set-dependent structural features (scaffolds) to the descriptor set as well as remove redundant structural features from the descriptor set. Once a preliminary descriptor set has been created, an automatic descriptor selection procedure in LPDM selects the top 30% descriptors according to Yates X^2 -test for a binary response variable. A predictive model for a binary response variable is built using partial logistic regression (PLR) with further selection of descriptors in an iterative procedure, and selection of the optimum PLR factors based on least predictive residual sum of squares.

LPDM has the option of building composite binary models for training sets with a skewed distribution between the two activity classes, i.e. actives and inactives. With this option a number of sub-models are constructed, taking in each sub-model the entire smaller class, here the actives, and an equally large sample from the bigger class, here the inactives. The samples from the bigger class used in each of the sub-models are selected randomly but in such a way that their intersection is minimal and their union is the entire bigger class. The positive prediction probability (see Section 2.4) for a test chemical from a composite model is defined as the average of the positive prediction probabilities of all sub-models where the test chemical is in the structural domain [48]. Each sub-model in a composite model has its own unique set of selected descriptors and number of PLR factors.

We used five different modeling approaches in LPDM to build five predictive models for each of the four training sets: 1) single, 2) single with scaffolds, 3) single with scaffolds and reduced structural features, 4) composite, and 5) composite with scaffolds. In 1) and 4), the descriptors were selected among the default initial descriptor set, i.e. containing molecular descriptors and selected predefined structural features, and used to build a single model and a composite model, respectively. Next, scaffolds were generated in LPDM from the training set structures and added to the initial descriptor set, which subsequently was used for descriptor selection for models 2) and 5). In model 3), the scaffold-enriched descriptor set was reduced before descriptor selection by removing most similar structural features using a built-in function in LPDM. All models underwent a ten times two-fold cross-validation by the LPDM algorithm, which reuses the selected descriptor set from the parent model when building the cross-validation models [48]. For each of the four endpoints, we selected the predictive model with the highest performance from the LPDM cross-validation for further validation and screening studies (Fig. 1). The LPDM cross-validations were only applied for model selection and not used for model performance assessments. The four selected models were 'closed' for further development after this selection.

2.4. Applicability domain

Our definition of the applicability domain (AD) consists of two components: 1) the definition of a structural domain in LPDM, and 2) an in-house class probability refinement on the output from LPDM. For a test compound to be within LPDM's structural domain it is required that: all molecular descriptors used in the model can be calculated, it contains at least one structural feature used in the model, and that it has at least 30% Tanimoto similarity (default cut-off in the LPDM software) with a training set compound [48]. No prediction call (active/inactive) is generated by LPDM for a test compound outside this structural domain. For test compounds within the LPDM structural domain, a positive prediction probability, p , between 0 and 1, is given together with the prediction call; actives having a $p \geq 0.5$ and inactives having a $p < 0.5$ [48]. To

Table 1

Overview of the sizes of the training sets and the blinded external test sets used to develop and validate the four QSAR models. An extra dataset for hPXR-LBD binding was used for external validation. Substances with inconclusive experimental results were removed from the datasets.

Datasets	Training set			External test set		
	Total	Active (%)	Inactive (%)	Total	Active (%)	Inactive (%)
hPXR-LBD*	1537	143 (9.3)	1394 (90.7)	651	30 (4.6)	621 (95.4)
hPXR	1644	207 (12.6)	1437 (87.4)	702	59 (8.4)	643 (91.6)
rPXR	1671	97 (5.8)	1574 (94.2)	730	24 (3.3)	706 (96.7)
CYP3A4	1676	179 (10.7)	1497 (89.3)	715	45 (6.3)	670 (93.7)
Extra hPXR-LBD	–	–	–	2434	279 (11.5)	2155 (88.5)

* The experimental results of the test set were masked from the model developers at DTU Food by NIH NCATS until the models were developed and the test set had been predicted.

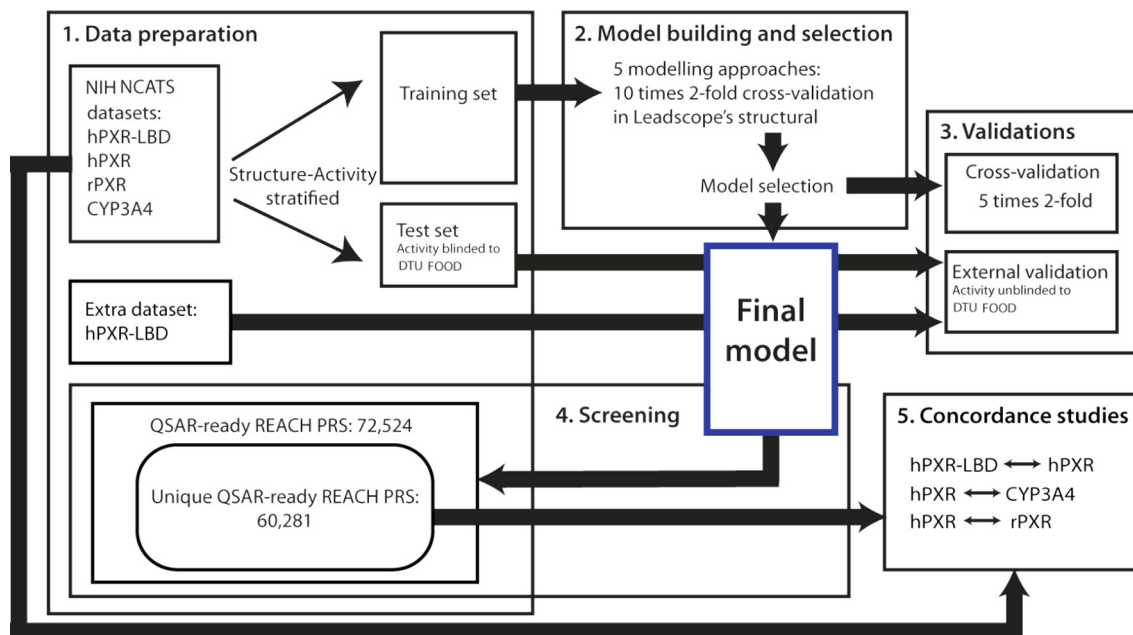


Fig. 1. Workflow of the modeling, screening and concordance rate studies.

exclude less reliable predictions, i.e. those with a positive prediction probability close to $p = 0.5$, we required $p \geq 0.7$ for active prediction calls and $p \leq 0.3$ for inactive prediction calls. Predictions within the LPDM structural domain but with an associated positive prediction probability in the interval 0.3 to 0.7 were defined as out of AD and excluded from the statistical analyses.

2.5. Cross- and external validation of the models

Each of the four selected predictive models was subsequently subject to a five times twofold stratified cross-validation procedure to estimate their robustness and predictive performance (Fig. 1). The applied procedure did not use the LPDM built-in cross-validation functionality. Instead, this was done by randomly removing 50% of the structures from the training set, keeping the ratio of actives and inactives. Then a cross-validation model was built from the reduced training set using the same modeling approach as in the parent model but by performing novel modeling where no information, such as selected descriptors, was reused from the parent model. The cross-validation model was applied to predict the removed 50%. Likewise, a cross-validation model was made on the removed 50% of the training set, and this model was used to predict the other 50%. This procedure was repeated five times resulting in ten cross-validation models. Sensitivity, specificity and balanced accuracy [49] were calculated for each of the ten cross-validation models, and from these the mean and standard deviation (SD) were computed to give an overall statistical estimate of the predictive performance and robustness of the full-training set parent model. Sensitivity is the percentage of experimental actives correctly predicted, specificity is the percentage of the experimental inactives correctly predicted, and balanced accuracy is the average of the sensitivity and specificity [49]. The coverage, i.e. the mean percentage of how many of the predicted substances that had predictions within the AD of the ten cross-validation models, was also calculated.

In addition, all four models underwent a blinded external validation using the experimentally masked test sets to further evaluate their predictive performance (Fig. 1). The prediction calls within the AD were compared to the experimental results, which

were made available to DTU Food by NIH NCATS after the model building step was finalized and the test sets predicted. The hPXR-LBD model underwent an additional external validation with the extra test set for hPXR-LBD. This external validation was not blinded, however, the data set was not applied in any of the model development or selection steps. Coverage, sensitivity, specificity and balanced accuracy were calculated for each model.

2.6. Screening of the REACH PRS inventory

The four selected and validated QSAR models were used to predict the activity of 72,524 substances from the REACH PRS list (Fig. 1). The REACH PRS chemical structures were extracted from the online Danish (Q)SAR Database structure set [44,45]. The structures were originally curated from deliverable 3.4 of the OpenTox EU project [39] and had been processed through the same structure preparation steps as described in Section 2.2 to meet the structural requirements from the QSAR modeling software. The proportion of the QSAR-predicted REACH PRS within the AD of each of the four models as well as the activity distributions of the predictions was calculated.

2.7. Concordance rates between endpoints

To study the co-occurrences in positive results for PXR binding, PXR activation and CYP3A4 induction, positive concordance rates both ways between the following endpoints were estimated:

- hPXR-LBD and hPXR,
- hPXR and rPXR, and
- hPXR and CYP3A4.

This was done for the full experimental drug datasets, i.e. the training and external test set data (excluding the extra hPXR-LBD test set) combined, as well as for the 60,281 unique structures out of the 72,524 QSAR-ready REACH PRS (Fig. 1).

For any endpoints, A and B, we used the following definition of the rate of actives in A also active in B, denoted *Concordance rate* ($A \rightarrow B$):

Concordance rate($A \rightarrow B$)

$$= \frac{\# \text{active in } A \text{ AND } B}{\# \text{active in } A \text{ AND } B + \# \text{active in } A \text{ AND in active in } B}$$

We apply the above definition twice for each pair of endpoints, A and B, to calculate *Concordance rate* ($A \rightarrow B$) and *Concordance rate* ($B \rightarrow A$).

For example, to assess the rate of hPXR-LBD ligands that activate hPXR, the following calculation was made:

Concordance rate(hPXR – LBD \rightarrow hPXR)

$$= \frac{\# \text{predicted/tested active in hPXR-LBD AND hPXR}}{\# \text{predicted/tested active in hPXR-LBD AND hPXR} + \# \text{predicted/tested active in hPXR – LBD AND in active in hPXR}}$$

Likewise, the concordance rate for hPXR activators that were also active for binding to hPXR-LBD was calculated as:

Concordance rate(hPXR \rightarrow hPXR – LBD)

$$= \frac{\# \text{predicted/tested active in hPXR-LBD AND hPXR}}{\# \text{predicted/tested active in hPXR – LBD AND hPXR} + \# \text{predicted/tested active in hPXR AND in active in hPXR-LBD}}$$

Differences and similarities between corresponding concordance rates in the drug and REACH PRS universes were identified.

3. Results

3.1 Predictive performance and robustness

For each of the four endpoints the model with the highest performance from the LPDM cross-validation was selected for further validation and screening studies. The four selected models were all composite models consisting of seven to ten sub-models. Each of the four selected models underwent both an in-house rigorous five times leave-50%-out cross-validation and a DTU Food blinded external validation to assess their robustness and predictive performance within the defined AD. The validation results are presented in Table 2 together with information about the number of sub-models in the selected composite model. Overall, the results presented in Table 2 show that the rigorous leave-50%-out cross-validations underestimated the models' predictive performances compared to the blinded external validations. The models will be made available for prediction of user-submitted structures in a coming free online Danish (Q)SAR Models sister-site to the Danish (Q)SAR database at the DTU homepage [45].

3.2. Screening of the REACH PRS inventory

A set of 72,524 substances from the REACH PRS list was screened through the four QSAR models. Of the 72,524 REACH PRS, 28.6% (20,727) were in the common AD of all four models, and of these, 1.5% corresponding to 320 substances were predicted active for all four endpoints and 77.1% corresponding to 15,979 substances were predicted inactive by all four models. The number of REACH PRS predicted within the defined AD of each model and the distribution of active and inactive predictions are given in Table 3.

3.3. Concordance rates between hPXR-LBD binding and Full-Length hPXR activation

The cell-free hPXR-LBD assay is a LanthaScreen TR-FRET (time resolved fluorescence resonance energy transfer)-based assay that identifies binding of a chemical to the LBD of human PXR, whereas the cell-based hPXR assay identifies compounds that can activate human full-length PXR either through direct LBD binding or through other signaling pathways [50,51]. In order to obtain more

information on frequencies of possible mechanisms of PXR activation for drugs and REACH PRS, we calculated two-way concordance

rates between hPXR-LBD binding and full-length hPXR activation for the experimental results of the full drug datasets and for the QSAR predictions of the REACH sets, respectively (Fig. 2a). For the experimental drug data the rate of hPXR-LBD tested binders resulting in hPXR activation was 44.0% (63/(63 + 79)), and the rate of hPXR activators binding to hPXR-LBD was 37.7% (63/(63 + 104)). For the predicted REACH substances only compounds in the common AD of the two models (n = 22,486) were included in the analysis, and among these 2624 were predicted active by both models and 16,842 were predicted inactive by both models. Of the remaining 3020 discordant predictions, 2408 were predicted active for hPXR-LBD but inactive for hPXR, while 612 were predicted active for hPXR but inactive for hPXR-LBD. Based on these predictions, it was estimated that 52.1% (2624/(2,624 + 2408)) of the predicted hPXR-LBD actives are also predicted to cause hPXR activation, whereas 81.1% (2624/(2,624 + 612)) of the predicted hPXR activators are also predicted to bind to hPXR-LBD.

3.4. Concordance rates between hPXR activation and CYP3A4 induction

Since PXR is known to induce the transcription of CYP3A4 [4,31], we calculated the concordance rates between hPXR activation and CYP3A4 induction for both the tested drugs and the QSAR-predicted REACH substances set (Fig. 2b). For the experimental drug data, the rate of hPXR active drugs that result in CYP3A4 induction was 53.6% (113/(113 + 98)), and the rate of CYP3A4 inducers also activating hPXR was 66.5% (113/(113 + 57)). Of the 24,364 REACH PRS predicted within the common AD of the two models, 2945 were predicted active by both models, whereas 20,960 were predicted inactive in both models. Among the 459 substances with discrepant predictions, 385 were predicted active by hPXR only and 74 were predicted active only by the CYP3A4 model. From these numbers it can be estimated that 88.4% (2945/(2945 + 459)) of the REACH substances predicted to cause hPXR activation were also predicted to induce CYP3A4, and that 97.5% (2945/(2945 + 74)) of the predicted CYP3A4 inducing REACH substances were also predicted to activate hPXR.

Table 2

Coverage and predictive performance of the four QSAR models. Only predictions inside the defined AD were included in the statistical analyses.

QSAR model	Statistical parameter	Cross-validation,% (SD,%)	External validation,% (actual numbers)	
		5 times 2-fold*	Blinded test sets**	Extra hPXR-LBD test set
hPXR-LBD Approach 5) 10 sub-models	Coverage	66.0 (3.3)	67.3 (438/651)	60.6 (1475/2434)
	Sensitivity	68.7 (7.3)	85.0 (17/20)	71.9 (97/135)
	Specificity	84.5 (2.0)	87.8 (367/418)	80.4 (1078/1340)
	Balanced accuracy	76.6 (3.2)	86.4	76.1
hPXR Approach 5) 7 sub-models	Coverage	60.3 (2.9)	59.1 (415/702)	–
	Sensitivity	72.5 (6.7)	80.0 (24/30)	–
	Specificity	80.4 (3.7)	85.2 (328/385)	–
	Balanced accuracy	76.4 (2.9)	82.6	–
rPXR Approach 4) 10 sub-models	Coverage	74.0 (3.0)	80.0 (584/730)	–
	Sensitivity	58.9 (11.0)	91.3 (21/23)	–
	Specificity	92.0 (2.4)	94.1 (528/561)	–
	Balanced accuracy	75.4 (4.7)	92.7	–
CYP3A4 Approach 5) 9 sub-models	Coverage	64.7 (3.0)	63.4 (453/715)	–
	Sensitivity	71.6 (7.6)	76.9 (20/26)	–
	Specificity	80.7 (2.7)	85.5 (365/427)	–
	Balanced accuracy	76.1 (3.3)	81.2	–

* A five times twofold cross-validation with same active-inactive ratio as the full training set and without reusing selected descriptors from the parent model. Coverage, sensitivity and specificity are the mean from the ten cross-validation models with the standard deviation (SD) in parentheses.

** The experimental results of the test set structures were made available to DTU Food by NIH NCATS after they had been predicted in the respective models by DTU Food.

Table 3

Prediction and domain results for the 72,524 REACH PRS.

QSAR model	Total in AD (%)	Predicted Active in AD (%)	Predicted Inactive in AD (%)
hPXR-LBD	43,551 (60.1)	11,490 (26.4)	32,061 (73.6)
hPXR	38,114 (52.5)	6167 (16.2)	31,947 (83.8)
rPXR	52,144 (71.9)	3141 (6.0)	49,003 (94.0)
CYP3A4	42,861 (59.1)	5874 (13.7)	36,987 (86.3)

3.5. Concordance rates between human and rat Full-Length PXR activation

Species differences in PXR activation by chemicals have previously been identified [11,14,52] and information on these differences can be of importance when extrapolating data from rat *in vivo* studies to humans, e.g. in chemical risk assessment. In the experimental drug dataset, the rate of human PXR activating drugs that also activate the rat PXR was 25.9% (51/(51 + 146)) (Fig. 2c). Conversely, 56.7% (51/(51 + 39)) of the rat PXR activating drugs also activated human PXR. To estimate the species differences in human and rat PXR activation with regard to the QSAR-predicted REACH substances, we compared REACH PRS QSAR-predictions from the hPXR and rPXR models. Among the 25,498 REACH PRS predicted in the common AD, 862 were predicted active in both models, 2788 were predicted active for hPXR only, and 573 were predicted active for rPXR only. The remaining 21,275 were predicted inactive by both models. From this it can be estimated that 23.6% (862/(862 + 2788)) of the QSAR-predicted REACH PRS activating human PXR were also predicted to activate rat PXR, and 60.1% (862/(862 + 573)) of the predicted rat PXR activators were also predicted as human PXR activators.

4. Discussion

In the present study, we developed four global binary QSAR models for human PXR-LBD binding, human and rat full-length PXR activation, and human CYP3A4 induction, respectively. The models were used to screen more than 70,000 REACH substances. To our knowledge this is the first study to profile a large set of chemical substances potentially used in industrial processes, food and consumer products, such as cleaning products, paints, clothes,

and furniture, by QSAR with respect to both PXR binding/activation and CYP3A4 induction.

4.1. Predictive performance and robustness

A number of different modeling approaches in LPDM were used to build models on the four training sets and the best performing model for each endpoint was selected for further validation studies and screening of the REACH PRS inventory. It is known that sensitivity and specificity of binary models can, depending on the applied modeling algorithm, be affected by the distribution of actives and inactives in the training set. A training set with a greater number of inactives will often result in a higher specificity at the expense of sensitivity and vice versa in the case of overrepresentation of actives. This is likely the reason why the single models built with the full, imbalanced training sets were outperformed by the composite models: all four selected models were composite models consisting of seven to ten sub-models with balanced sub-training sets. The composite model feature in LPDM was implemented to handle imbalanced training sets [48], in this case training sets with only 5.8% to 12.6% actives.

All four models showed high predictive performances with balanced accuracies in the external validations ranging from 76.1% to 92.7% (Table 2). Both the high quality of the experimental data originating from robust assays [14,53] as well as the composite modeling approach in LPDM have undoubtedly contributed to the high performances of the models. The cross-validation results were generally pessimistic compared to the external validations (Table 2), especially with regard to the sensitivity. The fact that the cross-validation results in this study are pessimistic compared to the external validations is in accordance with the finding in, e.g. [54], where this issue was systematically studied. The generally low standard deviations (SDs) in the cross-validations indicate robust models, i.e. their performances are not drastically altered in response to perturbations of the training set composition. Both the remarkably lower cross-validation sensitivities relative to the external validation sensitivities and their higher SDs is likely due to the rigorous cross-validation procedure of removing 50% of the few actives in the non-congeneric training sets. The effects of removing 50% is most clearly reflected in the rPXR model (Table 2), which was also the model with the fewest training set actives, i.e. 97 actives (Table 1). Often *k*-fold cross-validations of models built from training sets of similar size as those in this study are

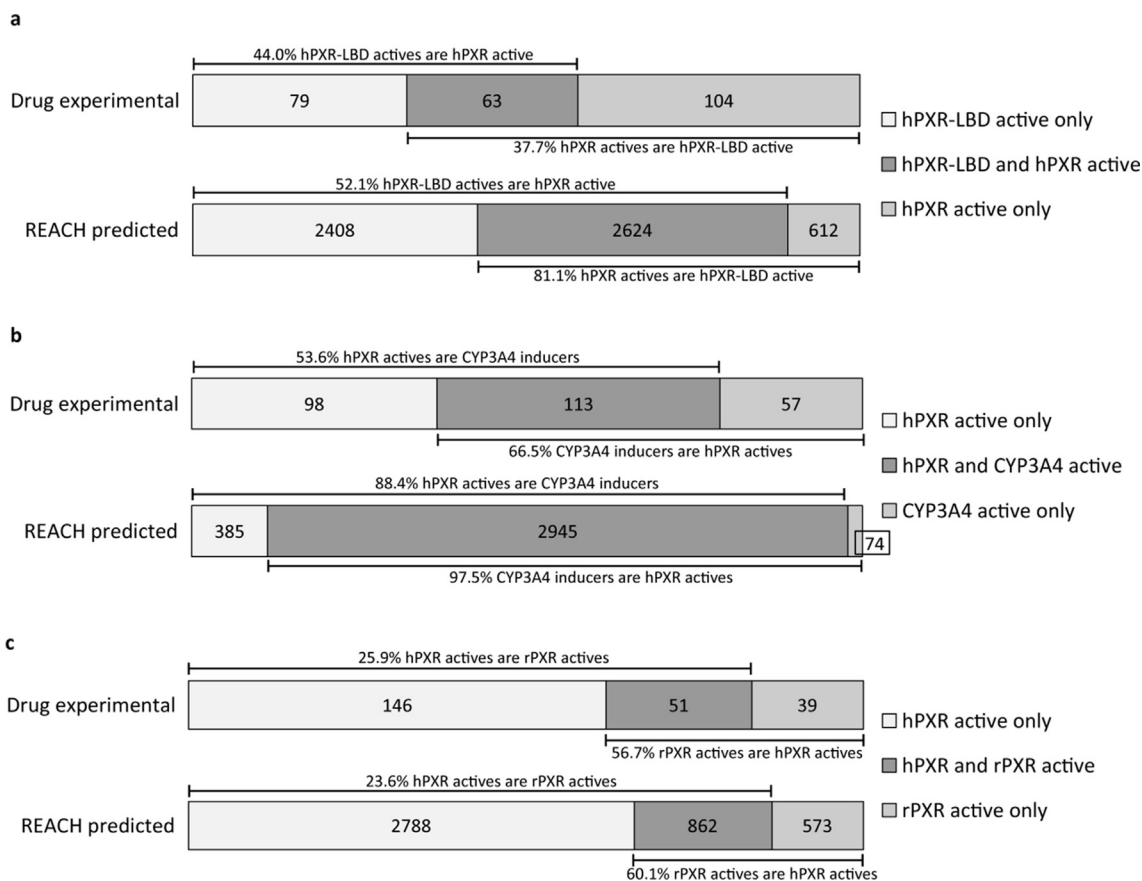


Fig. 2. Overlap of positive results between two endpoints and two-way concordance rates. a) comparing tested/predicted hPXR-LBD binders with hPXR activators, b) comparing tested/predicted hPXR activators with CYP3A4 inducers, and c) comparing tested/predicted rPXR activators with hPXR activators.

performed by removing 10% or 20% (i.e., $k = 10$ or 5) of the training set, leaving more data to train the cross-validation models [52,54]. The cross-validation results indicate that the leave-50%-out cross-validation performed in the present study was causing too big perturbations. Retrospectively, it seems that a 10 or 20%-leave-out cross-validation would have been more appropriate in this case.

The hPXR-LBD model in the present study has a lower cross-validation sensitivity (68.7%) compared to a similar hPXR-LBD model from Dybdahl and colleagues (82.3%) [14,20,43]. The difference in sensitivities is likely due to differences in the composition of the two training sets, with the Dybdahl model having more than twice as many actives in its training set, i.e. 299 versus 143 actives in the current model, leaving more actives for the 50% reduced cross-validation models. Additionally, the Dybdahl model cross-validation [20] was performed using LPDMs algorithm, which, we have experienced in some cases, returns overoptimistic statistics because of its reuse of parent model descriptors in the cross-validation models.

The size of the DTU Food masked external test sets with predictions inside the respective model's AD ranged from 415 to 584 structures, with 20–30 structures having active experimental results (Table 2). In general, external test sets should be sufficiently large and representative of the model's AD to ensure that the predictive performance results are not random. The distributions of experimentally active and inactive structures in these external test sets are imbalanced toward more inactives similar to the training set distributions. Although the masked test sets in total are quite large for external validation, the few actives make the calculations of sensitivity less robust. The supplementary external validation of the hPXR-LBD model included 135 experimentally active sub-

stances out of the total 1475 test set structures predicted inside the hPXR-LBD model's AD (Table 2). This larger number of actives may provide a more accurate estimate of the hPXR-LBD model's sensitivity compared to the result from the blinded external validation with only 20 experimentally active compounds. The extra external validation of the hPXR-LBD model resulted in overall lower predictive performance estimates compared to the blinded external validation (Table 2). This can be due to differences in the chemical universes of the two test set with the blinded test set likely representing the training set better due to the chemical-similarity test set selection procedure described in Section 2.1 [55,56]. A previous study have shown that this type of rational test set selection can give optimistic validation results [57]. Also, although the hPXR-LBD data in the two datasets were generated using the same assay protocol in the same laboratory, minor differences in the data analysis of the extra hPXR-LBD dataset compared to that of the NIH NCATS hPXR-LBD data could have negatively affected the validation results to some degree. Available ToxCast datasets [34] with experimental results for human PXR binding and activation and CYP3A4 induction were not applied in the validation study due, in our opinion, to large dissimilarities in the assay protocols and data analysis with the NIH NCATS training sets.

4.2. Screening of the REACH PRS inventory

The four selected models were used to predict 72,524 REACH PRS in order to give an estimate of the number of PXR activators and CYP3A4 inducers in this chemical universe (Table 3). A large overlap in the chemical similarity of small molecule drugs and

environmental chemicals has been identified, and other QSAR models trained on drug data have been shown to have a high predictability of environmental chemicals [52,55,56]. This, together with the application of a structural AD to avoid extrapolations, justifies the use of the drug-data trained models to screen the REACH set. The screening indicates that the predicted REACH PRS set contains nearly the same rate of human and rat PXR full-length activators as well as CYP3A4 inducers compared to the experimentally tested drugs in the training sets, i.e. 16% vs. 13%, 6% vs. 5.8%, and 14% vs. 11%, respectively. The hPXR-LBD model, however, predicted 26% of the REACH PRS inside the model's AD to be hPXR-LBD ligands, which was remarkably higher than the 9.3% hPXR-LBD active drugs in the training set. Since the hPXR-LBD model does not seem to be biased towards producing many false positive predictions based on the high specificity in the three validations, i.e. 80.4% to 87.8% (Table 2), this is unlikely the only reason for the high prevalence of predicted hPXR-LBD actives in the REACH PRS set. The increased focus on attenuation of PXR activity and the introduction of a filtering procedure in early drug development [30] might to some degree explain the nearly three-fold lower rate of hPXR-LBD ligands among drugs compared to the predicted REACH substances.

4.3. Concordance rates between endpoints

The calculated concordance rates between endpoints using either experimental test results or QSAR predictions can provide information on the frequencies of the possible mechanisms by which chemicals act as well as reveal differences and similarities between the two chemical inventories (Fig. 2). Results from a previous study indicate that differences in the biological mechanisms of drugs and environmental chemicals exist [58]. When concordance rates are based on QSAR predictions, they can be influenced by the uncertainty inherent in the predictive models, but since all four models had high predictive performances in the external validations (Table 2), we expect this uncertainty to be fairly low. For the concordance rates based on the experimental data, these can be affected by the fact that experimental tests may not be 100% reproducible. In a follow-up study, Shukla and colleagues [14] retested 72 compounds in the four qHTS assays and the activities were confirmed for 71 (hPXR-LBD), 66 (hPXR), 72 (rPXR) and 70 (CYP3A4) of the compounds, respectively, with no information of the activity distribution. This could indicate a slightly higher rate of false positive and/or false negative test results in the hPXR assay compared to the other three assays. Inclusion of false positives and/or negatives in the hPXR experimental data could in this case have affected the hPXR model development and its performance measurements as well as the subsequent concordance rate studies of both the experimental and predicted datasets.

Roughly half of the hPXR-LBD binders were also hPXR activators for both the tested drugs (44%) and the predicted REACH PRS (52%) (Fig. 2a). This may reflect that the ~50% active compounds from the hPXR-LBD cell-free assay that are not active in the cell-based hPXR activation assay either cannot enter the cell, are biodegraded in the cellular environment, or act as human PXR antagonists [14,28]. For the hPXR activators that were also hPXR-LBD ligands, we observed a difference in the concordance rates between the two universes, with only 38% of the full-length hPXR activators being hPXR-LBD ligands for the tested drugs as opposed to 81% for the QSAR-predicted REACH PRS. This difference might be a reflection of the approximately three-times higher occurrence of predicted hPXR-LBD binders in the QSAR-predicted REACH PRS universe and thus a higher chance for hPXR activators to also be predicted active by hPXR-LBD. The part of the hPXR activators that were not hPXR-LBD ligands likely exert their effect on PXR activation through other signaling pathways such as protein kinase path-

ways [50,51]. They may also be chemicals that are not able to displace the tracer molecule in the hPXR-LBD assay [14], a known problem with LanthaScreen TR-FRET-based binding assays.

When comparing hPXR activation and CYP3A4 induction higher concordance rates were found for the QSAR-predicted REACH PRS than for the tested drugs (Fig. 2b). Among the REACH PRS predictions, 88.4% of the hPXR activators also induced CYP3A4, while for the experimentally tested drugs this was only the case for 53.5% of the hPXR activators. Multiple factors can explain the absence of CYP3A4 induction by hPXR activators, for example, negative feedback loops repressing CYP3A4 expression, differences in recruitment of co-activators resulting in variations in the promoter region binding and downstream gene transcription patterns [59], as well as assay-related biochemical limitations [60]. Of the CYP3A4 inducers, 97.5% and 66.5% of the predicted REACH PRS and tested drugs, respectively, were also hPXR activators. An explanation to why some CYP3A4 inducers were not hPXR activators could be that other transcription factors or signaling pathways in the cell have led to the CYP3A4 induction. The high concordance rates of 97.5% and 88.4% between the prediction sets indicate that the two models have high agreement in their predictions.

Previous studies have reported species differences between human and rat PXR ligands [14,15,52,61] and this is supported by a highly divergent inter-species PXR-LBD amino acid sequence [11] with human and rat PXR-LBD sharing only 78.3% amino acid sequence similarity according to a calculation made using the web-based SeqAPASS software [62]. In the present study, around 25% of the hPXR activators among both the tested drugs and the predicted REACH PRS were also activating rPXR (Fig. 2c). Among the rPXR activators 57–60% in both universes were also activating hPXR. These results support that species differences in chemical action of drugs and REACH substances on PXR exist. The current study has identified 3361 (2788 + 573) REACH substances for which extra attention is necessary when extrapolating rat *in vivo* data to humans.

Overall, this statistical analysis indicates that QSAR predictions of larger chemical inventories can be applied to study overlap in activities between biological endpoints. Such studies can potentially be used in hypotheses generation of new mechanistic associations.

5. Conclusions

We have developed four QSAR models for human PXR-LBD binding, human and rat full-length PXR activation, and human CYP3A4 induction. All four models were robust with high predictive performances. The models were used to screen a set of 72,524 REACH PRS and of the QSAR-predicted REACH substances the number of actives were as follows; hPXR-LBD (11,490), hPXR (6167), rPXR (3141), and CYP3A4 (5874). Furthermore, the experimental data and the predictions of the REACH substances were analyzed to obtain information on co-occurrences of positive results for PXR activation and CYP3A4 induction in the two chemical universes. The developed models can in a fast and cost-efficient way provide information that can be used for prioritization purposes as well as in combination with other data in IATAs including weight-of-evidence assessments of chemical substances. The models can also help in future design of safer chemicals and drugs.

Conflict of interest statement

The authors declare that they have no conflict of interest in relation with this paper.

Acknowledgements

We would like to thank the Danish 3R Center and the Danish Environmental Protection Agency for supporting the project.

References

- [1] D.J. Mangelsdorf, C. Thummel, M. Beato, P. Herrlich, G. Schütz, K. Umesono, B. Blumberg, P. Kastner, M. Mark, P. Chambon, R.M. Evans, The nuclear receptor superfamily: the second decade, *Cell* 83 (1995) 835–839, [http://dx.doi.org/10.1016/0092-8674\(95\)90199-X](http://dx.doi.org/10.1016/0092-8674(95)90199-X).
- [2] A. di Masi, E. De Marinis, P. Ascenzi, M. Marino, Nuclear receptors CAR and PXR: molecular, functional, and biomedical aspects, *Mol. Aspects Med.* 30 (2009) 297–343, <http://dx.doi.org/10.1016/j.mam.2009.04.002>.
- [3] S.A. Kliewer, J.T. Moore, L. Wade, J.L. Staudinger, M.A. Watson, S.A. Jones, D.D. McKee, B.B. Oliver, T.M. Willson, R.H. Zetterström, T. Perlmann, J.M. Lehmann, An orphan nuclear receptor activated by pregnanes defines a novel steroid signaling pathway, *Cell* 92 (1998) 73–82, [http://dx.doi.org/10.1016/S0092-8674\(00\)80900-9](http://dx.doi.org/10.1016/S0092-8674(00)80900-9).
- [4] G. Bertilsson, J. Heidrich, K. Svensson, M. Åsman, L. Jendeborg, M. Sydow-Backman, R. Ohlsson, H. Postlind, P. Blomquist, A. Berkenstam, Identification of a human nuclear receptor defines a new signaling pathway for CYP3A induction, *Proc. Natl. Acad. Sci.* 95 (1998) 12208–12213, <http://dx.doi.org/10.1073/pnas.95.21.12208>.
- [5] J.M. Lehmann, D.D. McKee, M.A. Watson, T.M. Willson, J.T. Moore, S.A. Kliewer, The human orphan nuclear receptor PXR is activated by compounds that regulate CYP3A4 gene expression and cause drug interactions, *J. Clin. Invest.* 102 (1998) 1016–1023, <http://dx.doi.org/10.1172/JCI3703>.
- [6] A.H. Tolson, H. Wang, Regulation of drug-metabolizing enzymes by xenobiotic receptors: PXR and CAR, *Adv. Drug Deliv. Rev.* 62 (2010) 1238–1249, <http://dx.doi.org/10.1016/j.addr.2010.08.006>.
- [7] C. Xu, C.Y.-T. Li, A.-N.T. Kong, Induction of phase I, II and III drug metabolism/transport by xenobiotics, *Arch. Pharm. Res.* 28 (2005) 249–268, <http://dx.doi.org/10.1007/BF02977789>.
- [8] D. Gardner-Stephen, J.-M. Heydel, A. Goyal, Y. Lu, W. Xie, T. Lindblom, P. Mackenzie, A. Radominska-Pandya, Human PXR variants and their differential effects on the regulation of human UDP-glucuronyltransferase gene expression, *Drug Metab. Dispos.* 32 (2004) 340–347, <http://dx.doi.org/10.1124/dmd.32.3.340>.
- [9] R.E. Watkins, G.B. Wisely, L.B. Moore, J.L. Collins, M.H. Lambert, S.P. Williams, T.M. Willson, S.A. Kliewer, M.R. Redinbo, The human nuclear xenobiotic receptor PXR: structural determinants of directed promiscuity, *Science* (80-) 292 (2001) 2329–2333, <http://dx.doi.org/10.1126/science.1060762>.
- [10] V. Delfosse, B. Dendele, T. Huet, M. Grimaldi, A. Boulahtouf, S. Gerbal-Chaloin, B. Beucher, D. Roeklin, C. Müller, R. Rahmani, V. Cavailès, M. Daujat-Chavanieu, V. Vivat, J.M. Pascucci, P. Balaguer, W. Bourguet, Synergistic activation of human pregnane X receptor by binary cocktails of pharmaceutical and environmental compounds, *Nat. Commun.* 6 (2015) 1–10, <http://dx.doi.org/10.1038/ncomms9089>.
- [11] S.A. Jones, L.B. Moore, J.L. Shenk, G.B. Wisely, G.A. Hamilton, D.D. McKee, N.C.O. Tomkinson, E.L. LeCluyse, M.H. Lambert, T.M. Willson, S.A. Kliewer, J.T. Moore, The pregnane X receptor: a promiscuous xenobiotic receptor that has diverged during evolution, *Mol. Endocrinol.* 14 (2000) 27–39, <http://dx.doi.org/10.1210/mend.14.1.0409>.
- [12] H. Zhang, E. LeClyse, L. Liu, M. Hu, L. Matoney, W. Zhu, B. Yan, Rat pregnane X receptor: molecular cloning, tissue distribution, and xenobiotic regulation, *Arch. Biochem. Biophys.* 368 (1999) 14–22, <http://dx.doi.org/10.1006/abbi.1999.1307>.
- [13] E.L. LeCluyse, Pregnane X receptor: molecular basis for species differences in CYP3A induction by xenobiotics, *Chem. Biol. Interact.* 134 (2001) 283–289, [http://dx.doi.org/10.1016/S0009-2797\(01\)00163-6](http://dx.doi.org/10.1016/S0009-2797(01)00163-6).
- [14] S.J. Shukla, S. Sakamuru, R. Huang, T.A. Moeller, P. Shinn, D. VanLeer, D.S. Auld, C.P. Austin, M. Xia, Identification of clinically used drugs that activate pregnane X receptors, *Drug Metab. Dispos.* 39 (2011) 151–159, <http://dx.doi.org/10.1124/dmd.110.035105>.
- [15] Y. Sui, S.-H. Park, R.N. Helsley, M. Sunkara, F.J. Gonzalez, A.J. Morris, C. Zhou, Bisphenol A increases atherosclerosis in pregnane X receptor-humanized ApoE deficient mice, *J. Am. Hear. Assoc.* 3 (2014) 1–11, <http://dx.doi.org/10.1161/JAHA.113.000492>.
- [16] E.J. Squires, T. Sueyoshi, M. Negishi, Cytoplasmic localization of pregnane X receptor and ligand-dependent nuclear translocation in mouse liver, *J. Biol. Chem.* 279 (2004) 49307–49314, <http://dx.doi.org/10.1074/jbc.M407281200>.
- [17] M.N. Jacobs, G.T. Nolan, S.R. Hood, Lignans, bacteriocides and organochlorine compounds activate the human pregnane X receptor (PXR), *Toxicol. Appl. Pharmacol.* 209 (2005) 123–133, <http://dx.doi.org/10.1016/j.taap.2005.03.015>.
- [18] X.C. Kretschmer, W.S. Baldwin, CAR and PXR: xenosensors of endocrine disruptors?, *Chem. Biol. Interact.* 155 (2005) 111–128, <http://dx.doi.org/10.1016/j.cbi.2005.06.003>.
- [19] N.K. Chaturvedi, S. Kumar, S. Negi, R.K. Tyagi, Endocrine disruptors provoke differential modulatory responses on androgen receptor and pregnane and xenobiotic receptor: potential implications in metabolic disorders, *Mol. Cell. Biochem.* 345 (2010) 291–308, <http://dx.doi.org/10.1007/s11010-010-0583-6>.
- [20] M. Dybdahl, N.G. Nikolov, E.B. Wedebye, S.O. Jónsdóttir, J.R. Niemelä, QSAR model for human pregnane X receptor (PXR) binding: screening of environmental chemicals and correlations with genotoxicity, endocrine disruption and teratogenicity, *Toxicol. Appl. Pharmacol.* 262 (2012) 301–309, <http://dx.doi.org/10.1016/j.taap.2012.05.008>.
- [21] I. Shah, K. Houck, R.S. Judson, R.J. Kavlock, M.T. Martin, D.M. Reif, D.J. Dix, Using nuclear receptor activity to stratify hepatocarcinogens, *PLoS ONE* 6 (2011) e14584, <http://dx.doi.org/10.1371/journal.pone.0014584>.
- [22] AOP-wiki, AOP-Wiki homepage, 2016. https://aopwiki.org/wiki/index.php/Main_Page (accessed October 6, 2016).
- [23] AOP:8, Aop:8 – Upregulation of Thyroid Hormone Catabolism via Activation of Hepatic Nuclear Receptors, and Subsequent Adverse Neurodevelopmental Outcomes in Mammals, 2016. <https://aopwiki.org/wiki/index.php/Aop:8> (accessed October 6, 2016).
- [24] G.T. Ankley, R.S. Bennett, R.J. Erickson, D.J. Hoff, M.W. Hornung, R.D. Johnson, D.R. Mount, J.W. Nichols, C.L. Russom, P.K. Schmieder, J.A. Serrano, J.E. Tietge, D.L. Villeneuve, Adverse outcome pathways: a conceptual framework to support ecotoxicology research and risk assessment, *Environ. Toxicol. Chem.* 29 (2010) 730–741, <http://dx.doi.org/10.1002/etc.34>.
- [25] S. Gutsell, P. Russell, The role of chemistry in developing understanding of adverse outcome pathways and their application in risk assessment, *Toxicol. Res. (Camb.)* 2 (2013) 299, <http://dx.doi.org/10.1039/c3tx50024a>.
- [26] N.C. Kleinstreuer, K. Sullivan, D. Allen, S. Edwards, D.L. Mendrick, M. Embry, J. Matheson, J.C. Rowlands, S. Munn, E. Maull, W. Casey, Adverse outcome pathways: from research to regulation scientific workshop report, *Regul. Toxicol. Pharmacol.* 76 (2016) 39–50, <http://dx.doi.org/10.1016/j.yrtph.2016.01.007>.
- [27] K.E. Tollefson, S. Scholz, M.T. Cronin, S.W. Edwards, J. de Knecht, K. Crofton, N. Garcia-Reyero, T. Hartung, A. Worth, G. Patlewicz, Applying adverse outcome pathways (AOPs) to support integrated approaches to testing and assessment (IATA), *Regul. Toxicol. Pharmacol.* 70 (2014) 629–640, <http://dx.doi.org/10.1016/j.yrtph.2014.09.009>.
- [28] S. Ekins, C. Chang, S. Mani, M.D. Krasowski, E.J. Reschly, M. Iyer, V. Kholodovych, N. Ai, W.J. Welsh, M. Sinz, P.W. Swaan, R. Patel, K. Bachmann, Human pregnane X receptor antagonists and agonists define molecular requirements for different binding sites, *Mol. Pharmacol.* 72 (2007) 592–603, <http://dx.doi.org/10.1124/mol.107.038398>.
- [29] E. Qiao, M. Ji, J. Wu, R. Ma, X. Zhang, Y. He, Q. Zha, X. Song, L.-W. Zhu, J. Tang, Expression of the PXR gene in various types of cancer and drug resistance (Review), *Oncol. Lett.* 5 (2013) 1093–1100, <http://dx.doi.org/10.3892/ol.2013.1149>.
- [30] Y. Gao, S.H. Olson, J.M. Balkovec, Y. Zhu, I. Royo, J. Yabut, R. Evers, W. Tang, D.P. Hartley, R.T. Mosley, S.H. Olson, J.M. Balkovec, Y. Zhu, I. Royo, J. Yabut, R. Evers, E.Y. Tan, W. Tang, D.P. Hartley, R.T. Mosley, Attenuating pregnane X receptor (PXR) activation: a molecular modelling approach, *Xenobiotica* 37 (2007) 124–138, <http://dx.doi.org/10.1080/00498250601050412>.
- [31] M. Sinz, G. Wallace, J. Sahi, Current industrial practices in assessing CYP450 enzyme induction: preclinical and clinical, *AAPS* 10 (2008) 391–400, <http://dx.doi.org/10.1208/s12248-008-9037-4>.
- [32] J.E. Laine, S. Auriola, M. Pasanen, R.O. Juvonen, Acetaminophen bioactivation by human cytochrome P450 enzymes and animal microsomes, *Xenobiotica* 39 (2009) 11–21, <http://dx.doi.org/10.1080/00498250802512830>.
- [33] D.J. Dix, K.A. Houck, M.T. Martin, A.M. Richard, R.W. Setzer, R.J. Kavlock, The ToxCast program for prioritizing toxicity testing of environmental chemicals, *Toxicol. Sci.* 95 (2007) 5–12, <http://dx.doi.org/10.1093/toxsci/kfl103>.
- [34] ToxCast, iCSS ToxCast Dashboard, 2016. <https://actor.epa.gov/dashboard/> (accessed October 13, 2016).
- [35] K.L. Dionisio, A.M. Frame, M.-R. Goldsmith, J.F. Wambaugh, A. Liddell, T. Cathey, D. Smith, J. Vail, A.S. Ernstoff, P. Fantke, O. Joliet, R.S. Judson, Exploring consumer exposure pathways and patterns of use for chemicals in the environment, *Toxicol. Reports* 2 (2015) 228–237, <http://dx.doi.org/10.1016/j.toxrep.2014.12.009>.
- [36] P.P. Egeghy, R. Judson, S. Gangwal, S. Mosher, D. Smith, J. Vail, E.A. Cohen, Hubal, The exposure data landscape for manufactured chemicals, *Sci. Total Environ.* 414 (2012) 159–166, <http://dx.doi.org/10.1016/j.scitotenv.2011.10.046>.
- [37] ECHA, Guidance on information requirements and chemical safety assessment, 2008. https://echa.europa.eu/documents/10162/13632/information_requirements_r6_en.pdf (accessed December 8, 2016).
- [38] OECD, Guidance Document on the Validation of (Quantitative) Structure-Activity Relationship [(Q)SAR] Models, 2, 2007, pp. 1–154. [http://www.oecd.org/officialdocuments/publicdisplaydocumentpdf/?cote=env/jm/mono\(2007\)2&doclanguage=en](http://www.oecd.org/officialdocuments/publicdisplaydocumentpdf/?cote=env/jm/mono(2007)2&doclanguage=en) (accessed December 8, 2016).
- [39] OpenTox, Final database with additional content, 2011. <http://opentox.org/data/documents/development/opentoxreports/opentoxreportd34/view> (accessed October 14, 2016).
- [40] Reach, Regulation (EC) No 1907/2006 of the European Parliament and of the Council of 18 December 2006, Off. J. Eur. Communities. L 269, 2006, pp. 1–15. <http://eur-lex.europa.eu/legal-content/EN/TXT/HTML/?uri=CELEX:02006R1907-20140410&from=EN> (accessed October 14, 2016).
- [41] C.L. Mellor, F.P. Steinmetz, M.T.D. Cronin, Using molecular initiating events to develop a structural alert based screening workflow for nuclear receptor ligands associated with hepatic steatosis, *Chem. Res. Toxicol.* 29 (2016) 203–212, <http://dx.doi.org/10.1021/acs.chemrestox.5b00480>.
- [42] R. Huang, N. Southall, Y. Wang, A. Yasgar, P. Shinn, A. Jadhav, D.-T. Nguyen, C.P. Austin, The NCGC pharmaceutical collection: a comprehensive resource of

- clinically approved drugs enabling repurposing and chemical genomics, *Sci. Transl. Med.* 3 (2011) 80ps16, <http://dx.doi.org/10.1126/scitranslmed.3001862>.
- [43] S.J. Shukla, D.-T. Nguyen, R. MacArthur, A. Simeonov, W.J. Frazee, T.M. Hallis, B. D. Marks, U. Singh, H.C. Eliason, J. Printen, C.P. Austin, J. Inglese, D.S. Auld, Identification of pregnane X receptor ligands using time-resolved fluorescence resonance energy transfer and quantitative high-throughput screening, *Assay Drug Dev. Technol.* 7 (2009) 143–169, <http://dx.doi.org/10.1089/adt.2009.193>.
- [44] QSAR, User Manual for the Danish (Q)SAR Database, 2015. http://qsardb.food.dtu.dk/Danish_QSAR_Database_Draft_User_manual.pdf (accessed October 14, 2016).
- [45] QSARDB, Danish (Q)SAR Database, 2015. <http://qsar.food.dtu.dk/> (accessed October 14, 2016).
- [46] Leadscope, Leadscope, Inc, 2016. <http://www.leadscope.com/> (accessed October 14, 2016).
- [47] G. Roberts, G.J. Myatt, W.P. Johnson, K.P. Cross, P.E. Blower, LeadScope \ddagger : software for exploring large sets of screening data, *J. Chem. Inf. Comput. Sci.* 40 (2000) 1302–1314, <http://dx.doi.org/10.1021/ci0000631>.
- [48] L.G. Valerio, C. Yang, K.B. Arvidson, N.L. Kruhlak, A structural feature-based computational approach for toxicology predictions, *Expert Opin. Drug Metab. Toxicol.* 6 (2010) 505–518, <http://dx.doi.org/10.1517/17425250903499286>.
- [49] J.A. Cooper II, R. Saracci, P. Cole, Describing the validity of carcinogen screening tests, *Br. J. Cancer.* 39 (1979) 87–89.
- [50] X. Ding, J.L. Staudinger, Repression of PXR-mediated induction of hepatic CYP3A gene expression by protein kinase C, *Biochem. Pharmacol.* 69 (2005) 867–873, <http://dx.doi.org/10.1016/j.bcp.2004.11.025>.
- [51] W. Lin, J. Wu, H. Dong, D. Bouck, F. Zeng, T. Chen, Cyclin-dependent kinase 2 negatively regulates human pregnane X receptor-mediated CYP3A4 gene expression in HepG2 liver carcinoma Cells^{*}, *J. Biol. Chem.* 283 (2008) 30650–30657, <http://dx.doi.org/10.1074/jbc.M806132200>.
- [52] M.D.M. AbdulHameed, D.L. Ippolito, A. Wallqvist, Predicting rat and human pregnane X receptor activators using bayesian classification models, *Chem. Res. Toxicol.* (2016), <http://dx.doi.org/10.1021/acs.chemrestox.6b00227>.
- [53] F.P. Steinmetz, S.J. Enoch, J.C. Madden, M.D. Nelms, N. Rodriguez-sanchez, P.H. Rowe, Y. Wen, M.T.D. Cronin, Methods for assigning confidence to toxicity data with multiple values — Identifying experimental outliers, *Sci. Total Environ.* 482–483 (2014) 358–365, <http://dx.doi.org/10.1016/j.scitotenv.2014.02.115>.
- [54] M. Gütlein, C. Helma, A. Karwath, S. Kramer, A large-scale empirical evaluation of cross-validation and external test set validation in (Q)SAR, *Mol. Inform.* 32 (2013) 516–528, <http://dx.doi.org/10.1002/minf.201200134>.
- [55] B.L. Ingle, B.C. Veber, J.W. Nichols, R. Tornero-Velez, Informing the human plasma protein binding of environmental chemicals by machine learning in the pharmaceutical space: applicability domain and limits of predictability, *J. Chem. Inf. Model.* (2016), <http://dx.doi.org/10.1021/acs.jcim.6b00291>.
- [56] Y. Yin, D.T. Chang, C.M. Grulke, Y.-M. Tan, M.-R. Goldsmith, R. Tornero-Velez, Essential set of molecular descriptors for ADME prediction in drug and environmental chemical space, *Research.* (2014), <http://dx.doi.org/10.13070/rs.en.1.996>.
- [57] T.M. Martin, P. Harten, D.M. Young, E.N. Muratov, A. Golbraikh, H. Zhu, A. Tropsha, Does rational selection of training and test sets improve the outcome of QSAR modeling?, *J. Chem. Inf. Model.* 52 (2012) 2570–2578, <http://dx.doi.org/10.1021/ci300338w>.
- [58] F. Shah, N. Greene, Analysis of Pfizer compounds in EPA's ToxCast chemicals-assay space, *Chem. Res. Toxicol.* 27 (2014) 86–98, <http://dx.doi.org/10.1021/tx400343t>.
- [59] C.-H. Ngan, D. Beglov, A.N. Rudnitskaya, D. Kozakov, D.J. Waxman, S. Vajda, The structural basis of pregnane X receptor binding promiscuity, *Biochemistry* 48 (2009) 11572–11581, <http://dx.doi.org/10.1021/bi901578n>.
- [60] G. Luo, M. Cunningham, S. Kim, T. Burn, J. Lin, M. Sinz, G. Hamilton, C. Rizzo, S. Jolley, D. Gilbert, A. Downey, D. Mudra, R. Graham, K. Carroll, J. Xie, A. Madan, A. Parkinson, D. Christ, B. Selling, E. LeCluyse, L.-S. Gan, CYP3A4 induction by drugs: correlation between a pregnane X receptor reporter gene assay and CYP3A4 expression in human hepatocytes, *Drug Metab. Dispos.* 30 (2002) 795–804, <http://dx.doi.org/10.1124/dmd.30.7.795>.
- [61] T.A. Kocarek, E. Schuetz, P. Guzelian, Regulation of phenobarbital-inducible cytochrome P450 2B1/2 mRNA by lovastatin and oxysterols in primary cultures of adult rat hepatocytes, *Toxicol. Appl. Pharmacology.* 120 (1993) 298–307, <http://dx.doi.org/10.1006/taap.1993.1115>.
- [62] C.A. LaLone, D.L. Villeneuve, D. Lyons, H.W. Helgen, S.L. Robinson, J.A. Swintek, T.W. Saari, G.T. Ankley, Sequence alignment to predict across species susceptibility (SeqAPASS): a web-based tool for addressing the challenges of cross-species extrapolation of chemical toxicity, *Toxicol. Sci.* 153 (2016) 228–245, <http://dx.doi.org/10.1093/toxsci/kfw119>.